Adenosine conformations of nucleotides bound to methionyl tRNA synthetase by transferred nuclear Overhauser effect spectroscopy.

Nagarajan Murali, Y Lin, Yves Mechulam, Pierre Plateau, B. D. Nageswara Rao

Adenosine Conformations of Nucleotides Bound to Methionyl tRNA Synthetase by Transferred Nuclear Overhauser Effect Spectroscopy

Nagarajan Murali*, Yan Lin*, Yves Mechulam,# Pierre Plateau,# and B. D. Nageswara Rao*
*Department of Physics, Indiana University Purdue University Indianapolis, Indianapolis, Indiana 46202-3273, and #Laboratoire de Biochimie, Unite de Recherche Associee, au CNRS m° 1970, Ecole Polytechnique, 91128 Palaiseau, France

ABSTRACT The conformations of MgATP and AMP bound to a monomeric tryptic fragment of methionyl tRNA synthetase have been investigated by two-dimensional proton transferred nuclear Overhauser effect spectroscopy (TRNOESY). The sample protocol was chosen to minimize contributions from adventitious binding of the nucleotides to the observed NOE. The experiments were performed at 500 MHz on three different complexes, E · MgATP, E · MgATP · L-methioninol, and E · AMP · L-methioninol. A starter set of distances obtained by fitting NOE build-up curves (not involving H5′ and H5″) were used to determine a CHARMm energy-minimized structure. The positioning of the H5′ and H5″ protons was determined on the basis of a conformational search of the torsion angle to obtain the best fit with the observed NOEs for their superposed resonance. Using this structure, a relaxation matrix was set up to calculate theoretical build-up curves for all of the NOEs and compare them with the observed curves. The final structures deduced for the adenosine moieties in the three complexes are very similar, and are described by a glycosidic torsion angle (χ) of 56° ± 5° and a phase angle of pseudorotation (P) in the range of 47° to 52°, describing a $^3_4$T-$_4$E sugar pucker. The glycosidic torsion angle, χ, deduced here for this adenylyl transfer enzyme and those determined previously for three phosphoryl transfer enzymes (creatine kinase, arginine kinase, and pyruvate kinase), and one pyrophosphoryl enzyme (PRibPP synthetase), are all in the range 52° ± 8°. The narrow range of values suggests a possible common motif for the recognition and binding of the adenosine moiety at the active sites of ATP-utilizing enzymes, irrespective of the point of cleavage on the phosphate chain.

INTRODUCTION

ATP-utilizing enzymes occur in a large number of biochemical pathways and play a critical role in cellular processes. The most abundant among these are phosphoryl transfer enzymes (kinases), followed by adenylyl transfer enzymes, examples of which are the aminoacyl tRNA synthetases (activation reaction), and pyrophosphoryl transfer enzymes, such as 5-phospho-D-ribose 1-diphosphate (PRibPP) synthetase, which are relatively rare. The fact that the cleavage of ATP occurs at three different places in the triphosphate chain, and that all ATP-utilizing enzymes require Mg(II) in vivo as an obligatory component in the reaction complexes, makes the investigation of the active-site structures of these enzymes and their possible differentiation a subject of continued interest from the point of view of elucidating enzyme mechanisms.

A nucleotide in isolation has considerable internal mobility (Nageswara Rao and Ray, 1992), and the determination of its conformation in an enzyme complex requires rather detailed measurements. Recently the glycosidic orientation and sugar pucker of the adenosine moiety of ATP and ADP in their enzyme complexes has been characterized by the use of two-dimensional transferred nuclear Overhauser effect spectroscopy (TRNOESY) for a number of ATP-utilizing enzymes. The enzymes studied include three phosphoryl transfer enzymes, creatine kinase (Murali et al., 1993), pyruvate kinase (Jarori et al., 1994), arginine kinase (Murali et al., 1994), and one pyrophosphoryl transfer enzyme, PRibPP synthetase (Jarori et al., 1995). From the point of view of the TRNOESY methodology, these studies have clearly demonstrated the need for devising sample protocols that minimize weak nonspecific binding of the nucleotides, a factor that was ignored before these studies, to obtain reliable structures from the measurements. Furthermore, this improved methodology yielded nucleotide conformations described by a glycosidic orientation, χ, in the range 52° ± 8° for all of the enzymes, whether they catalyze phosphoryl transfer or pyrophosphoryl transfer. This naturally raises the question of whether this similarity is maintained by the adenylyl transfer enzymes such as the aminoacyl tRNA synthetases as well. The significance of this question is accentuated by the fact that the glycosidic orientations deduced from x-ray crystallography for nucleotides bound to kinases show disparate values, ranging from 10° for the AMP moiety of P^1,P^5-di(adenosine-5′) pentaphosphate (AP_5A) bound to adenylate kinase (Abele and Schulz, 1995) to 96° for MgAMPPNP bound to 3-phosphoglycerate kinase (McPhillips et al., 1996), in contrast with nearly equal values of obtained from NMR. A similar situation exists for the x-ray results for amino-acyl tRNA synthetases, with values of ranging from 32° for AMP bound to

Received for publication 30 October 1996 and in final form 6 February 1997.

Address reprint requests to Dr. B. D. Nageswara Rao, Department of Physics, Indiana University Purdue University Indianapolis, 402 North Blackford Street, Indianapolis, IN 46202-3273. Tel.: 317-274-6901; Fax: 317-274-2393; E-mail: brao@iupui.edu.

Dr. Murali's present address is Center for Interdisciplinary Magnetic Resonance, National High Magnetic Field Laboratory, 1800 E. Paul Dirac Dr., Tallahassee, FL 32310.

0006-3495/97/05/2275/10 $2.00

seryl tRNA synthetase (Belrhali et al., 1994) to 72° for ATP bound to aspartyl tRNA synthetase (Cavarelli et al., 1994).

An aminoacyl tRNA synthetase catalyzes the acylation of the respective tRNA in two steps as shown below (Meinnel et al., 1995; Fayat et al., 1980):

$$E + ATP + aa \xleftrightarrow{Mg^{(II)}} E \cdot aa - AMP + PP_i$$

$$E \cdot aa - AMP + tRNA^{aa} \leftrightarrow E + AMP + aa - tRNA^{aa},$$

where aa is the amino acid. In the first step (the activation reaction) the adenylyl transfer occurs from ATP. Three TRNOE studies of adenosine conformations in complexes of aminoacyl tRNA synthetases have been reported thus far. One of these studies was on MgATP bound to methionyl tRNA synthetase (MetRS, EC 6.1.1.10) in its native dimeric form, as well as to a tryptic fragment of MetRS, by Landy et al. (1992), and the other two were by Williams and Rosevear (1991a,b) on the inhibitor complexes of the MgATP analog, Mg(α,β-methylene) ATP, bound to a tryptic fragment of MetRS, and to isoleucyl tRNA synthetase, respectively. All the three enzymes were isolated from *Escherichia coli*. The glycosidic orientations deduced in these studies do not agree with the range given above, viz. 52° ± 8°. However, it may be noted that in any of these studies the effect of ligand concentrations on the observed NOEs were not explicitly determined to assess the role of adventitious nucleotide binding, although Williams and Rosevear (1991a) recognized that this might be an issue. The measurements of Williams and Rosevear (1991a,b) were analyzed on the basis of a two-spin approximation for delay times as large as 250 ms, for which it is not likely to be valid, although some indirect attempt was made in one of their studies (Williams and Rosevear, 1991a) to correct for spin-diffusion effects. In view of the recent demonstration that substantial contributions to the observed NOEs arise from adventitious binding, the conformation of the MgATP bound to these enzymes merits reinvestigation.

A two-dimensional TRNOESY investigation of the conformation of the adenosine moiety in the nucleotides MgATP and AMP bound to a fragment, M547, of MetRS is presented in this paper. The M547 fragment is a monomer of molecular mass 64 kDa with a single binding site for the nucleotides. The complexes studied were E · MgATP, E · MgATP · L-methioninol, and E · AMP · L-methioninol. L-methioninol is a substrate-analog inhibitor in the presence of which the nucleotide complexes are bound with enhanced affinity (Fayat et al., 1977). In particular, the dead-end complex, E · MgATP · L-methioninol, is thought to mimic the E · methionine · MgATP complex in the ground state. The sample protocol for all of these complexes was chosen such that weak nonspecific binding effects are minimized. The TRNOESY build-up curves were analyzed to obtain a starter set of distances, which were used as constraints in a CHARMm energy-minimization routine. The structure deduced by such an iterative combination of conformational search and energy minimization were used to compute theoretical build-up curves by using a relaxation matrix appropriate for fast exchange. The results obtained allow a comparison of the adenosine conformations obtained for the ATP and AMP complexes with the enzyme, as well as with those obtained for adenine nucleotides bound to the phosphoryl transfer and pyrophosphoryl transfer enzymes investigated earlier.

EXPERIMENTAL PROCEDURE

Materials

ATP and L-methioninol were obtained from Sigma Chemical Company (St. Louis, MO). Tris (hydroxymethyl) amino methane (deuterated-d_{11}) and 99.99% D_2O were supplied by Research Organics (Cleveland, OH). All other chemicals used were of analytical reagent grade.

Enzyme preparation

The truncated monomeric form of MetRS, M547, encoding the 547 N-terminal residues of the enzyme, was produced from the *metG*547 gene (Mellot et al., 1989). This gene was introduced in the pBSM547+ vector (Fourmy et al., 1993) under the control of the *lac* promoter. Production of the M547 enzyme in the presence of isopropylthiogalactoside (IPTG) (0.3 mM) was in JM101Tr cells (Hirel et al., 1988). The M547 enzyme was isolated to homogeneity by using two chromatographic steps as described previously (Meinnel et al., 1991): first on a Superose-6 molecular sieve (Pharmacia, 1.6 × 50 cm), and second on a Q-Hiload anion exchanger (Pharmacia, 1.6 × 10 cm, 2.5 ml/min, 100 mM/h KCl). Enzyme concentrations were determined using the specific extinction coefficient of 1.72 cm^2/mg at 280 nm for the trypsin-modified MetRS (Cassio and Waller, 1971).

Before making samples for the TRNOE experiments, the enzyme, which is normally stored at −20°C in 55% glycerol buffer with 10 mM mercaptoethanol, was reprecipitated by adding ammonium sulfate to 80% saturation. After centrifugation, the pellet was dissolved in 50 mM Tris-HCl (pH 8.0) containing 10 mM mercaptoethanol. The dissolved protein was extensively dialyzed against the same buffer to completely exchange out the glycerol in the enzyme solution. After dialysis the protein was concentrated using an Amicon concentrator, and 1 ml of the concentrated protein was subjected to block dialysis against 1 ml of 50 mM Tris-d_{11}-Cl buffer (pH 8.0), prepared in D_2O, containing 10 mM mercaptoethanol. At least 10 changes of Tris-d_{11}-Cl buffer were made to replace H_2O with D_2O. The enzyme was then centrifuged to discard any denatured protein before adding the nucleotides for the NMR experiments. The concentrations of the nucleotides were determined spectrophotometrically using the extinction coefficient $\epsilon_{259}^{mM} = 15.4\ cm^{-1}$.

NMR measurements

^1H NMR measurements were made on a Varian Unity 500 MHz NMR spectrometer. The typical sample protocol chosen for structure measurements contained 0.2 mM MetRS, 1 mM ATP, 5 mM $MgCl_2$, 3–4 mM L-methioninol, and 10 mM mercaptoethanol, buffered in 50 mM Tris-d_{11}-Cl (pH 8.0). Typical sample volumes were 600 μl. This protocol was arrived at by making TRNOE measurements as a function of ligand concentration to minimize effects from weak nonspecific binding of the nucleotides to the protein, as described in Results and Analysis. The solutions were in D_2O, and the sample temperature was maintained at 10°C. Magnesium ion concentrations were adequate for complete saturation of the nucleotide, as evidenced by the coalescence H5′ and H5″ resonances in the spectrum. The numbering of the different protons in the adenosine moiety is the same as in our earlier work (Murali et al., 1993, 1994; Jarori et al., 1994, 1995) and is schematically shown in Fig. 1.

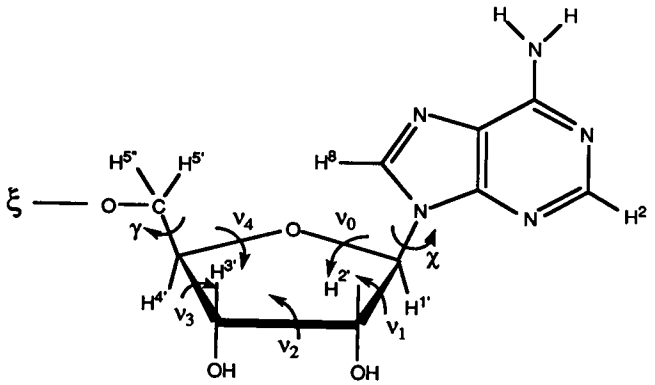

FIGURE 1 Adenosine moiety showing the numbering system used for the relevant protons.

NOESY (Kumar et al., 1980) time-domain data were collected in the hyper complex mode (States et al., 1982), with 256 increments and $2k$ data points during the acquisition period (t_2 dimension), for mixing times in the range of 35–250 ms. Thirty-two scans were averaged for each FID, and the zero-quantum interference was suppressed by random variation of the mixing time (up to 10% of its value) between different t_1 increments (Macura et al., 1981). A relaxation delay of 2 s was used, and the carrier frequency was placed at the solvent HDO resonance in all the experiments. The solvent HDO resonance was suppressed by monochromatic irradiation using the decoupler channel during intervals of the relaxation delay, the t_1 period, and the mixing period. Two-dimensional Fourier transformation was performed along both dimensions, with a shifted sine-bell apodization and zero filling to obtain a $2k$ (F1) × $4k$ (F2) data set. The spectra were phased to pure absorption mode. Fractional NOEs were determined by dividing the observed cross-peak volume by the diagonal-peak volume of H1′ extrapolated to zero mixing time. In experiments where the measurements were made only for a single mixing time (80 ms), a control spectrum was recorded with zero mixing time for the purpose of normalizing the NOEs as above.

Theoretical details

Because the dissociation constant of MgATP for MetRS is about 1–2 mM (Fayat and Waller, 1974), assuming that the on rate is diffusion controlled leads to an off rate of ~10^5 to 10^6 s^{-1} for the ligand in its enzyme complex, which is much larger than the typical NOE build-up rate ($\gamma^4\hbar^2\tau_c^b/10(r_{ij}^b)^6$) of ~450 s^{-1} (for r = 2.0 Å, τ_c = 50 ns). Thus the fast exchange condition is valid for these measurements. It has been shown that, in the limit of fast exchange, the intensity of the cross-peak in a TRNOESY experiment, representing polarization transfer from j to i, for a mixing time τ_m is given by

$$m_{i\leftarrow j}(\tau_m) = (e^{-\mathbf{R}\tau_m})_{ij} M_{0j} \quad (1)$$

$$= \left[1 - \mathbf{R}\tau_m + \frac{1}{2}\mathbf{R}^2\tau_m^2 - \frac{1}{6}\mathbf{R}^3\tau_m^3 + \ldots\right]_{ij} M_{0j}, \quad (2)$$

where $\mathbf{R}$ is the population-weighted average relaxation matrix of the bound and free complexes given by (Landy and Nageswara Rao, 1989)

$$\mathbf{R} = p_b\mathbf{W}^b + p_f\mathbf{W}^f, \quad (3)$$

in which p_b and p_f are bound and free fractional populations, and $\mathbf{W}^b$ and $\mathbf{W}^f$ are the corresponding relaxation matrices. Matrix elements of $\mathbf{W}^b$ and $\mathbf{W}^f$ are given by standard expressions for the case of dipolar interactions (Landy and Nageswara Rao, 1989; Kalk and Berendson, 1976; Keepers and James, 1984; Koning et al., 1990; Cambell and Sykes, 1991; Lee and Krishna, 1992). Equation 2 shows that the build-up of the intensity of a cross-peak given by $m_{i\leftarrow j}(\tau_m)$ versus τ_m in the TRNOESY spectrum is a polynomial in τ_m, and the initial slope of the build-up, which is just the linear term in Eq. 2, yields R_{ij}. Because the rotational correlation time, τ_c^b, for the bound nucleotide is considerably greater than that of the free nucleotide, τ_c^f, p_b/p_f is 0.1 to 0.25, and $(\omega\tau_c^b)^2 \gg 1$ (ω is the spectrometer frequency),

$$R_{ij} \approx p_b W_{ij} \approx -\frac{\gamma^4\hbar^2 p_b \tau_c^b}{10\,(r_{ij}^b)^6}. \quad (4)$$

Thus the ratios of initial slopes for different spin pairs are related to the corresponding internuclear distances in the bound conformation by

$$(R_{ij}/R_{lk}) \approx (r_{lk}^b/r_{ij}^b)^6. \quad (5)$$

An unknown distance r_{ij}^b can be estimated in terms of a calibration distance r_{ik}^b, with the help of Eq. 5, if such a distance can be identified within the spin system. Implicitly the calibration distance allows the evaluation of τ_c^b (more precisely, $p_b\tau_c^b$). Multiple-spin (or spin-diffusion) effects on the observed intensities arise from the quadratic and higher order terms in Eq. 2.

Molecular modeling and energy calculations

Molecular modeling and energy calculations were carried out using the CHARMm program (Brooks et al., 1983) in the software package QUANTA(4.1) running on a Silicon Graphics computer. The calculations were performed on an ATP/AMP molecule in vacuum. The distances derived from the NOEs were given as constraints for a symmetrical potential well with a force constant of 25 kcal/mol-Å^2 and an overall scale factor of 100 (the overall scale factor is a multiplication factor used in the CHARMm program for the NOE constraint potential). The energy was minimized by using the steepest-descent method.

RESULTS AND ANALYSIS

Ligand concentration dependence of NOE for MgATP complexes

TRNOESY experiments, each with a mixing time of 80 ms, were performed on a set of samples containing MetRS and MgATP, in which the ligand concentration was varied from 1 to 9 mM while keeping the ligand-to-enzyme concentration ratio fixed at a value of 10:1. The percentage TRNOE for the proton pair H1′-H2′ (this interproton distance remains practically unchanged, 2.9 ± 0.2 Å, for all sugar puckers and glycosidic torsions) obtained from these measurements is shown in Fig. 2 as a function of ligand concentration. The H1′-H2′ NOE starts at a value of ~1% for 1 mM ligand concentration, goes up to ~2% at 4 mM, and remains steady up to ~6 mM ligand concentration. A further increase of ligand concentration up to 9 mM increases the NOE to ~3.5%. The dissociation constant for MgATP binding with the tryptic fragment of MetRS was estimated to be ~1–2 mM (Fayat and Waller, 1974). Thus the first part of Fig. 2 is likely to have contributions from the progressive occupation of the specific MgATP-binding sites as well as that of some adventitious sites. The second part of Fig. 2 (after 6 mM) indicates the population of nonspecific interaction sites of k_d ~4–5 mM.

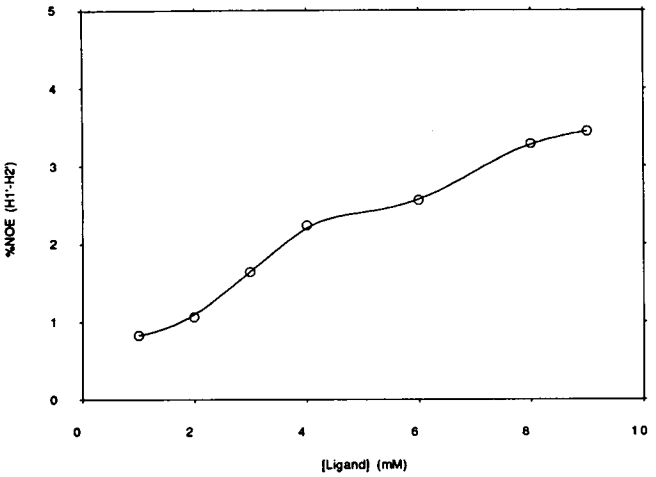

FIGURE 2 Dependence of percentage NOE for the H1′-H2′ proton pair on ATP concentration in E · MgATP complex. ATP concentration was varied from 1 to 9 mM, keeping the ATP-to-enzyme concentration ratio constant at 10:1. The sample was in 50 mM Tris-d_{11}-Cl and 10 mM mercaptoethanol at pH 8.0, and measurements were made at 500 MHz and 10°C with a mixing time of 80 ms. The NOEs were normalized by dividing the NOE peak volume with the diagonal peak volume of H1′ measured with zero mixing time.

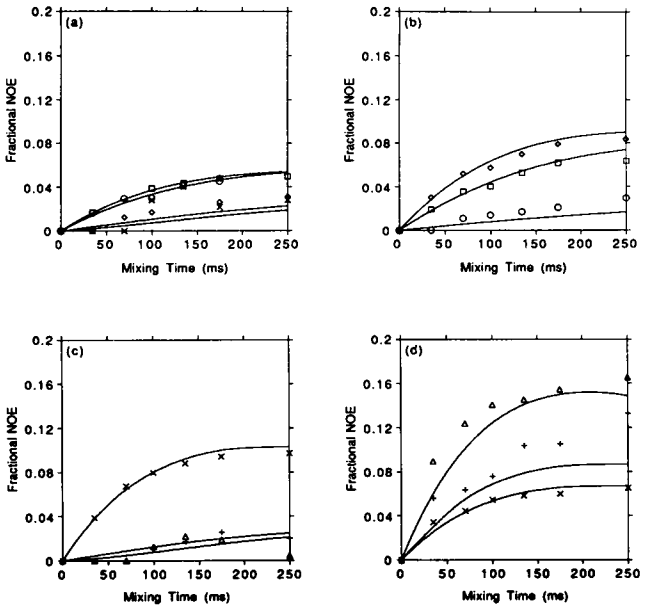

FIGURE 3 Percentage NOE build-up curves for E · MgATP complex. The sample contained 0.2 mM MetRs, 1.0 mM ATP, and 5 mM $MgCl_2$ in 50 mM Tris-d_{11}-Cl and 10 mM mercaptoethanaol at pH 8.0. NOEs for the proton pairs: (*a*) ○, H1′-H2′; ◇, H1′-H3′; □, H1′-H4′; ×, H1′-H5′/H5″. (*b*) ○, H8-H1′; □, H8-H2′; ◇, H8-H3′. (*c*) ×, H2′-H3′; +, H2′-H4′; △, H2′-H5′/H5″. (*d*) ×, H3′-H4′; +, H3′-H5′/H5″; △, H4′-H5′/H5″. The solid curves represent theoretically simulated build-up curves based on the relaxation matrix (Eq. 1) with the distances in Table 1. The external leakage rate used for all of the protons was 1.4 s^{-1}. The simulated NOEs for the distances involving H5′ and H5″ protons from a third proton were added and plotted along with the corresponding observed NOEs.

Intramolecular NOEs on enzyme-bound nucleotides

Based on the observation shown in Fig. 2, TRNOE measurements used for the determination of the conformation of the adenosine moiety of MgATP at the active site of the enzyme were performed at a nucleotide concentration of 1.0 mM and an enzyme concentration of 0.2 mM. The choice of the sample protocol is made to ensure a high occupancy of the active site and maximize the sensitivity of the observed NOE while keeping adventitious binding of MgATP with the enzyme minimal (see also Jackson et al., 1995). Another set of TRNOE measurements was made after the addition of 3.21 mM L-methioninol to the sample. The binding of MgATP to the enzyme is considerably enhanced in the presence of this substrate-analog inhibitor (Fayat et al., 1977). If the structures obtained for the two complexes are similar, it will provide useful corroborating evidence that adventitious binding effects are minimized under the chosen sample protocol.

When a sample protocol similar to the ATP complex above is used to form the E · AMP complex, no NOEs are observed, indicating very weak binding of AMP at the active site and the absence of nonspecific binding of AMP with the enzyme. The AMP measurements were performed, therefore, in the presence of L-methioninol, which is known also to increase the binding of AMP at the active site of this enzyme (Fayat et al., 1977). This was corroborated by the fact that measurable NOEs were observed in the presence of this substrate-analog inhibitor. The concentrations used for the E · AMP · L-methioninol complex were 0.142 mM enzyme, 1.47 mM AMP, and 2.93 mM L-methioninol. The experimental data of fractional NOEs are plotted as a function of the mixing time, τ_m, for the E · MgATP complex in Fig. 3, for the E · MgATP · L-methioninol complex in Fig. 4, and for the E · AMP · L-methioninol complex in Fig. 5. The solid curves are theoretical curves generated as described below.

Analysis of data and molecular modeling

As may be seen from Fig. 5, in the case of the AMP complex, NOE data are readily measurable only for five different proton pairs, viz. H1′-H2′, H1′-H4′, H8-H2′, H8-H3′, and H2′-H3′. These are the stronger NOEs in the data for the E · MgATP and E · MgATP · L-methioninol complexes as well (see Figs. 3 *a*, 3 *b*, 3 *c*, 4 *a*, 4 *b*, and 4 *c*). NOEs for the three proton pairs H3′-H4′, H3′-H5′/H5″, and H4′-H5′/H5″ (shown in Fig. 3 *d* for the E · MgATP complex and Fig. 4 *d* for the E · MgATP · L-methioninol complex) could not be measured with sufficient accuracy for the AMP complex because of the close proximity of H3′ and H4′ resonances in this case. Weak NOEs observed for the other proton pairs (H1′-H3′, H1′-H5′/H5″, H8-H1′, and H2′-H5′/H5″; see Figs. 3 *a*, 3 *b*, 3 *c*, 4 *a*, 4 *b*, and 4 *c*) in the E · MgATP and E · MgATP · L-methioninol complexes were too weak to measure in the case of the AMP complex.

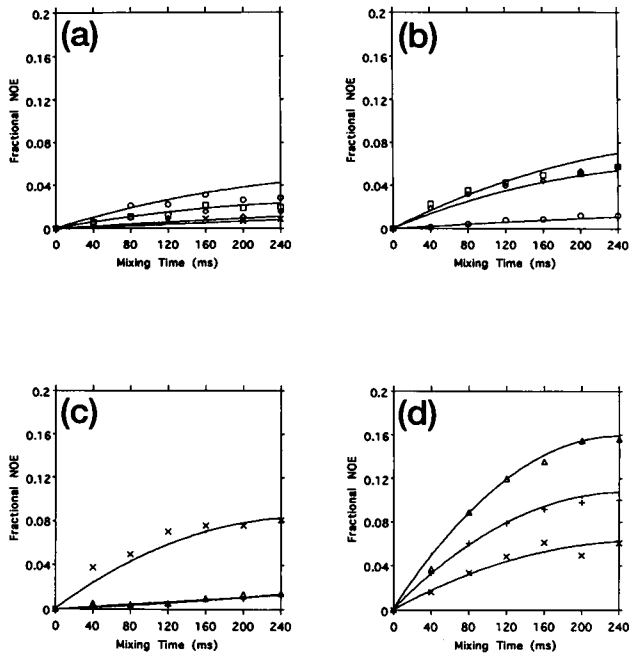

FIGURE 4 Percentage NOE build-up curves for E · MgATP · L-methioninol complex. The sample contained 0.20 mM MetRs, 1.07 mM ATP, 5 mM $MgCl_2$, and 3.21 mM L-methioninol in 50 mM Tris-d_{11}-Cl and 10 mM mercaptoethanol at pH 8.0. NOEs for the proton pairs: (*a*) ○, H1′-H2′; ◇, H1′-H3′; □, H1′-H4′; ×, H1′-H5′/H5″. (*b*) ○, H8-H1′; □, H8-H2′; ◇, H8-H3′. (*c*) ×, H2′-H3′; +, H2′-H4′; △, H2′-H5′/H5″. (*d*) ×, H3′-H4′; +, H3′-H5′/H5″; △, H4′-H5′/H5″. The solid curves represent theoretically simulated build-up curves based on the relaxation matrix (Eq. 1) with the distances in Table 1. The external leakage rate used for all of the protons was 1.4 s^{-1}. The simulated NOEs for the distances involving H5′ and H5″ protons from a third proton were added and plotted along with the corresponding observed NOEs.

To analyze the data obtained, an NOE calculation procedure, suitable for all of the complexes, has been devised along the following lines. The NOE build-up data for the proton pairs with strong NOEs, noted above, were fit with a second-order polynomial in τ_m (see Eq. 2). The initial slopes obtained from these fits were used along with Eq. 5 and a calibration distance of 2.9 Å for the H1′-H2′ distance (De Leeuw et al., 1980; Rosevear et al., 1983) to obtain a starter set of distances to be used for complete analysis of the data. The calibration distance also yields values of $p_b\tau_c^b$ appropriate for each complex. The distances obtained from strong NOEs for each complex were then used as unalterable constraints (upper limit and lower limit set equal to the targeted value) in the molecular modeling computations for the respective nucleotides, and the energies of the structures were minimized using the program CHARMm. Note, however, that distance constraints did not involve H5′ and H5″. Thus, even though these constraints were sufficient to determine the glycosidic torsion and some of the dihedral angles of the sugar pucker in the adenosine moiety, the torsion angle γ ($O_{5'}$-C'_5-C'_4-C'_3) was arbitrary. To determine the value of this angle that is compatible with the energy-minimized structures obtained above, a conformational search was set up in which γ was varied in the range of −180° to +180° in steps of 5°, and the CHARM energy was calculated for each structure. Furthermore, for each proton i that has observable NOEs with the superposed resonances of H5′ and H5″, an effective distance r_i from proton i is calculated. This distance (r_i) is given by $[(r_{1i}^{-6} + r_{2i}^{-6})/2]^{-1/6}$, corresponding to half the initial slope of the observed NOE, where r_{1i} and r_{2i} are distances of the proton i from H5′ and H5″. Note that r_i does not equal either r_{1i} or r_{2i}. In a relaxation matrix analysis, both of these distances may be replaced by r_i to obtain a correct measure of the superposed NOE. Thus the NOE analysis does not differentiate the two distances, and this can be accomplished only through energy minimization. Therefore, for each of the energy-minimized structures obtained from the conformational search in which γ is varied, the quantity $Q = \Sigma_i[(r_{1i}^{-6} + r_{2i}^{-6})/2r_i^{-6} - 1]^2$ is calculated. A range of values of γ that provides the best agreement with the observed NOEs of the superposed resonances of H5′ and H5″, i.e., the smallest value for Q, was then identified. The lowest-energy structure among these was then chosen as the structure for NOE calculation (see Eq. 3), along with the value $p_b\tau_c^b$ obtained from the calibration of the starter set of distances. The value of τ_c^b, assuming full occupancy of the enzyme site, obtained for all the three complexes is in the range of 14–21 ns. For free MgATP and AMP, a set of interproton distances representing an energy-minimized structure was used (Landy et al., 1992; Murali et al., 1993). External leakage rates of 1.4 s^{-1} were added to the diagonal elements of the relaxation matrices for all three complexes to fit the data for longer values of τ_m. Some variability in this parameter for different protons in a given complex cannot be ruled out. However, because there is no simple means of accurately differentiating the relaxation behavior of the different protons (for long delay times), a single leakage rate has been introduced for all of the protons. Energy minimization calculations performed for a given set of interproton distance constraints for the nucleotide with different initial coordinates yield virtually the same converged adenosine conformation. Although the distances deduced from strong NOEs (H1′-H2′, H1′-H4′, H8-H2′, H8-H3′, H2′-H3′ for both ATP and AMP complexes, and H3′-H4′ for ATP complexes only) were left unaltered in the computation, the distances obtained for the energy-minimized structures differ from those deduced for the weaker NOEs by less than 15%. By substituting these distances into relaxation matrices in Eq. 1, the theoretical NOE build-up curves were calculated for the three complexes. The build-up curves are plotted along with the experimental data as shown in Figs. 3, 4, and 5. The overall agreement between experimental and calculated NOE values is quite satisfactory.

The interproton distances representing the three structures are given in Table 1, and the various torsion angles in these structures are listed in Table 2. In all three complexes the glycosidic torsion angle (χ) for the adenosine moiety is about 56° ± 5°, corresponding to an *anti* conformation of the adenine base. The phase angle of pseudorotation (P) that

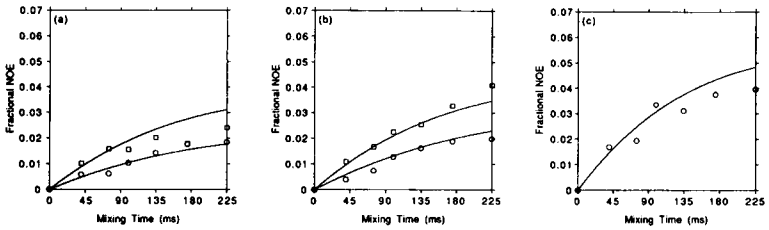

FIGURE 5 Percentage NOE build-up curves for E·AMP·L-methioninol complex. The sample contained 0.142 mM MetRs, 1.47 mM AMP, and 2.93 mM L-methioninol in 50 mM Tris-d_{11}-Cl and 5 mM mercaptoethanol at pH 8.0. NOEs for the proton pairs: (*a*) ○, H1′-H2′; □, H1′-H4′. (*b*) ○, H8-H2′; □, H8-H3′. (*c*) ○, H2′-H3′. The solid curves represent theoretically simulated build-up curves based on the relaxation matrix (Eq. 1) with the distances in Table 1. The external leakage rate used for all of the protons was 1.4 s^{-1}.

defines the sugar pucker (Altona and Sundaralingam, 1972; De Leeuw et al., 1980) is about 51° ($_4T^3$) for the E · MgATP complex, 47° ($_4T^3$) for the E · MgATP · L-methioninol complex, and 52° ($_4T^3$) for the E · AMP · L-methioninol complex. The corresponding amplitudes of sugar pucker $\tau = (\nu_2/\cos P)$ are 33°, 21°, and 44°, respectively. The adenosine conformation in the E · AMP · L-methioninol complex is depicted in Fig. 6. The other two structures are very similar to this diagram.

DISCUSSION

The reasoning behind the reinvestigation of the conformation of MgATP bound to MetRS was that previous TRNOE investigations have not explicitly scrutinized the role of adventitious binding of the nucleotide to the protein at places other than the active site, and the deduced structure may, therefore, be beset by errors introduced by such contributions. The results obtained for the ligand concentration dependence of NOE (see Fig. 2) show that this reasoning was correct. It is clear that at the MgATP concentrations (16 mM and 13 mM) employed by Landy et al. (1992), along with enzyme concentrations of 1–1.5 mM, there is considerable weak nonspecific binding of the nucleotide, and the NOEs observed in those experiments are primarily due to such binding and not to MgATP bound at the active site. Williams and Rosevear (1991a) used 0.2 mM enzyme and 3.0 mM ligand in their samples and obtained a value of 74° for χ in the Mg (α,β-methylene) ATP complex with a tryptic fragment of MetRS, and 81° for the same complex in the presence of L-methionine. Under the sample conditions used by Williams and Rosevear (1991a), weak nonspecific binding is expected to be minimal. However, there is another aspect of their methodology, viz., of using the two-spin approximation for data analysis, which involves some implicit and unverified assumptions. Williams and Rosevear (1991a) estimate that the effect of spin diffusion on their result generates an error of about 11% in their calculated distances. The discrepancy between the aforementioned values of χ deduced in their work and that obtained in the present work (~56°) may be due to a combination of several factors, such as adventitious binding of the ligand, methodology of NOE determination and analysis, and the

TABLE 1 Interproton distances in E · MgATP, E · MgATP · L-methioninol, and E · AMP · L-methioninol complexes, as determined by TRNOESY and energy minimization calculations

	r (Å)		
Proton pair	E · MgATP	E · MgATP · L-methioninol	E · AMP · L-methioninol
H1′-H2′	2.90	2.90	2.90*
H1′-H3′	3.71	3.92	3.80
H1′-H4′	2.82	3.19	2.64*
H1′-H5′	5.03	5.16	4.73
H1′-H5″	4.62	4.76	4.88
H2′-H3′	2.44	2.49	2.41*
H2′-H4′	3.60	3.82	3.75
H2′-H5′	4.84	4.78	5.41
H2′-H5″	5.39	5.34	4.63
H3′-H4′	2.61	2.64	3.06
H3′-H5′	2.57	2.42	2.39*
H3′-H5″	3.47	3.45	3.64*
H4′-H5′	2.57	2.52	2.96*
H4′-H5″	2.49	2.43	2.37*
H5′-H5″	1.81	1.75	1.81
H8-H1′	3.83	3.84	3.86
H8-H2′	2.80	2.71	2.84*
H8-H3′	2.57	2.78	2.60*
H8-H4′	4.37	4.48	4.59
H8-H5′	4.62	4.43	4.22*
H8-H5″	4.86	4.69	5.30*
H2-H8	6.46	6.46	6.46
H2-H1′	4.58	4.49	4.60
H2-H2′	6.05	6.12	6.15
H2-H3′	7.73	7.94	7.81
H2-H4′	7.39	7.65	7.21
H2-H5′	9.44	9.40	9.19
H2-H5″	8.85	8.78	9.10

For the E · MgATP complex, NOE constraints were used between H1′-H2′, H1′-H4′, H2′-H3′, H3′-H4′, H8-H2′, and H8-H3′. For the E · MgATP · L-methioninol and E · AMP · L-methioninol complexes, all of the above, except that between H3′-H4′, were used. The distances are given up to two significant decimal places, because premature rounding off may lead to artifactual deviations in NOE calculations. The values must be rounded off to one decimal place for model-building purposes. The uncertainty in distances is about ±0.20 Å.

*For the E · AMP · L-methioninol complex these are the proton pairs giving rise to observable NOEs. For the E · MgATP and E · MgATP · L-methioninol complexes, NOEs from all of the proton pairs, except for those involved with H2, are observable.

TABLE 2 Various dihedral angles and the pseudorotation phase angles *P* of MgATP and AMP bound at the active site of MetRS

Torsions	Angles (degrees)		
	E · MgATP	E · MgATP · L-methioninol	E · AMP · L-methioninol
$\chi(O_4' - C_1' - N_9 - C_8')$	53.5	58.6	55.0
$\nu_0(C_4' - O_4' - C_1' - C_2')$	−18.0	−10.4	−25.0
$\nu_1(O_4' - C_1' - C_2' - C_3')$	−2.6	−3.13	−3.5
$\nu_2(C_1' - C_2' - C_3' - C_4')$	21.0	14.5	27.6
$\nu_3(C_2' - C_3' - C_4' - O_4')$	−32.4	−20.9	−42.8
$\nu_4(C_3' - C_4' - O_4' - C_1')$	31.7	19.9	42.8
$\gamma(O_5' - C_5' - C_4' - C_3')$	80	80	120
$P = \tan^{-1}\frac{(\nu_4 + \nu_1) - (\nu_3 + \nu_0)}{2\nu_2(\sin 36° + \sin 72°)}$	50.9	47.2	51.6

For definitions used for various torsion angles, the torsion angle χ (O4′-C1′-N9-C8) is 0° when O4′-C1′ and N9-C8 bonds are eclipsed, and a counter-clockwise rotation about C1′-N9 bond is defined as a rotation by a positive angle. Because ν_2 is negative, 180° was added to the calculated value of *P* (see Altona and Sundaralingam, 1972).

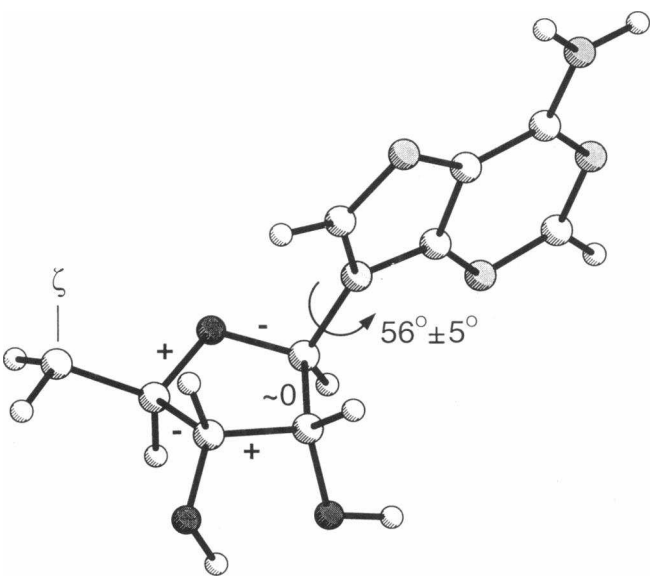

FIGURE 6 Pictorial representation of conformation of E · MgATP, E · MgATP · L-methioninol and E · AMP · L-methioninol bound at the active site of MTRS. (*a*) Glycosidic torsion angles and (*b*) the sign of various torsion angles defining the ribose conformation as well as the angle of pseudorotation (*P*) are given.

facile difference that a nucleotide-analog inhibitor complex has been used. The individual contributions of these different factors are a priori indeterminate, but together they are likely to account for the observed difference in the glycosidic orientations. It may be noted, nevertheless, that Williams and Rosevear (1991a) deduced the same sugar pucker ($_4^3$T-$_4$E) as in the present work, with a pseudorotation angle, *P*, in agreement with that given in Table 2 within experimental error.

The results of the present work corroborate and reiterate the need to deliberately minimize the contributions of adventitious binding in TRNOE determinations of structures of small molecules bound to macromolecules. This requirement is likely to be particularly stringent for charged ligands such as the nucleotides. The weak nonspecific binding of MgATP to the tryptic fragment of MetRS (molecular mass 64 kDa) was observed at ligand concentrations larger than about 5 mM. Smaller enzymes such as arginine kinase (40 kDa) (Murali et al., 1994), 3-P-glycerate kinase (47 kDa) (N. Murali, G. K. Jarori, and B. D. Nageswara Rao, unpublished results), and adenylate kinase (Y. Lin and B. D. Nageswara Rao, unpublished experiments) exhibit relatively minor adventitious binding effects. It appears, therefore, that TRNOE measurements of (nucleotide) complexes with heavy enzymes should be performed with the minimum ligand concentrations required for the feasibility of experimental measurements (~1 mM; Jarori et al., 1995), to ensure that the NOEs measured are specific to the active site.

The NOE calculation procedure used in analyzing the data is somewhat different from the iterative fit method used in our previous work (Murali et al., 1993, 1994; Jarori et al., 1994, 1995). However, the results obtained are quite satisfactory. This method is particularly suitable if the measurable NOEs are significantly fewer than the number of proton pairs, as in the case for the E · AMP · L-methioninol complex. Because there are many more NOEs observed for the MgATP complex than for the AMP complex, we also analyzed the data for this complex with the iterative-fitting procedure used in our earlier work by adjusting the structural parameters in a relaxation matrix to obtain the best agreement with the experiment. Such NOE-determined distances were subsequently used as constraints with an allowance of ±5% in a CHARMm energy-minimization routine. The procedure yielded virtually the same structure as that obtained with the NOE calculation method for the MgATP complex (see Table 1). This is a useful, although not unexpected, result, indicating the appropriateness of the analysis used.

In general, for structure determinations from TRNOESY measurements potential problems may arise from finite on-off rates, ligand motions at the active site, ligand-protein cross-relaxation, and protein-mediated spin diffusion (Ni and Zhu, 1994; Moseley et al., 1995; Jackson et al., 1995; Zheng and Post, 1993). Comparison of the exchange rates with cross-relaxation rates shows that the fast exchange condition is valid for the complexes studied here (*vide*

infra). ^{13}C lineshape studies of [2-^{13}C]ATP bound to various ATP-utilizing enzymes provide evidence that the bound nucleotide is immobilized in these complexes (Nageswara Rao and Ray, 1992). The analysis of the data in the present work is, however, limited by the lack of any specific information on ligand-protein cross-relaxation and protein-mediated spin-diffusion effects. Previous determinations of adenosine conformations indicate that these factors effectively reduce the value of τ_c^b appropriate for NOE build-up (Murali et al., 1993, 1994; Jarori et al., 1994, 1995). However, reasonable and internally consistent conformations could be deduced from the NOE data, presumably because the ratios of the cross-relaxation rates, and therefore interproton distances, are unaffected by a change in the rotational correlation times. In the complexes of MetRS studied in the present work, the values of τ_c^b inferred from the NOE build-up curves, by assuming full occupancy of the enzyme sites, are in the range of 14–21 ns smaller than the rotational correlation time expected for a molecular mass of 64 kDa, which is about 30 ns. The difference is probably not serious, in view of the uncertainty in the full-occupancy assumption. The similarity in the two values suggests that the protein-mediated spin diffusion is not as significant in these complexes as it was for those of the heavier enzymes studied previously. In those cases (Murali et al., 1993; Jarori et al., 1994, 1995), τ_c^b values obtained from the NOE analysis were considerably smaller (by a factor of 5 or more) than those estimated on the basis of the molecular mass of the respective proteins.

The glycosidic torsion angles, χ, and the phase angles of pseudorotation, P, describing sugar pucker, obtained for nucleotide complexes of all the ATP-utilizing enzymes investigated in the last few years are listed in Table 3. All of these structures were determined with methodology optimized both from NMR and biochemical points of view. A significant feature of the data in Table 3 is that the glycosidic torsion angles for all the complexes listed are in the range 52° ± 8°, irrespective of whether the enzymes catalyze phosphoryl transfer, pyrophosphoryl transfer, or adenylyl transfer, and whether the nucleotide is an ATP, ADP, or AMP. There are three phosphoryl transfer enzymes in the list, and there is one each representing the adenylyl transfer and pyrophosphoryl transfer enzymes. This is in contrast with a range of values of χ deduced in previously published work (Rosevear et al., 1981, 1983, 1987; Williams and Rosevear, 1991a,b). Sequence homologies are recently being discovered by x-ray crystallographic methods for nucleotide-binding sites (Higgins et al., 1986; Schulz, 1992; Hountondji et al., 1993; Traut, 1994; Smith and Rayment, 1996). Homologous sequences at the active site may, in general, be compatible with a number of heterogeneous conformations of the enzyme-bound nucleotides in the solid state. However, the narrow range of values for the glycosidic orientation obtained in our work for a disparate group of adenine nucleotide complexes in aqueous solutions is suggestive of a general feature related to the recognition and binding of the adenosine moiety in ATP-utilizing enzymes.

TABLE 3 Glycosidic torsion angles (χ), phase angles of pseudorotation (P), amplitude of sugar pucker (τ), along with sugar pucker designation (Altona and Sunderalingam, 1972; Sanger, 1984) for the adenosine moieties in nucleotide complexes of various ATP-utilizing enzymes obtained by TRNOESY methodology

Complex	χ (deg)	P (deg)	τ (deg)	Sugar pucker
ArgK · MgADP*	51	92.9	45.2	$^{\circ}E$
ArgK · MgADP · NO_3^- · Arg*	52	133.8	27.1	$_1E-^2_1T$
ArgK · MgATP*	50	130.8	28.9	$_1E-^2_1T$
CK · MgADP#	51	70.5	26.9	^2_4T
CK · MgATP#	51	70.5	26.9	^2_4T
PyK · MgATP (active site)§	44	42.4	28.4	$^3_4T-_4E$
PyK · MgATP (ancillary)§	46	127.6	22.1	$_1E-^2_1T$
PRPPS · MgATP‖	50	114.9	20.9	$^{\circ}_1T-_1E$
MetRS · MgATP¶	54	50.9	33.3	$^3_4T-_4E$
MetRS · MgATP · L-methioninol¶	59	47.2	21.3	$^3_4T-_4E$
MetRS · AMP · L-Methioninol¶	55	51.6	44.4	$^3_4T-_4E$
Free ATP*	5	29.0	35.1	$^3E-^3_4T$

The values for an energy-minimized structure of free ATP are included for comparison. The enzymes are abbreviated as ArgK (arginine kinase), CK (creatine kinase), PyK (pyruvate kinase), and PRPPS (PRibPP synthetase).
*Murali et al. (1994).
#Murali et al. (1993).
§Jarori et al. (1994).
‖Jarori et al. (1995).
¶Present work.

The values of the phase angle of pseudorotation listed in Table 3, however, vary over an appreciable range from ~40° to 130°. The variation occurs between different nucleotide complexes of the same enzyme or between complexes of a given nucleotide with different enzymes. There are no discernible systematics in the sugar puckers in these enzyme-nucleotide complexes, in contrast with the narrow range of values for the glycosidic torsion angle, χ, in all of these different complexes.

Aminoacyl tRNA synthetases are divided into two classes that differ by mutually exclusive sets of sequence motifs (Eriani et al., 1990), and in the hydroxyl specificity of tRNA aminoacylation (Hecht, 1979). There are 10 aminoacyl tRNA synthetases of class I, including MetRS. It is interesting to inquire whether there are any distinguishing features in the bound nucleotide conformation in these two classes. Toward such a goal, we are currently making TRNOESY measurements on the nucleotide complexes of lysyl tRNA synthetase, which belongs to class II.

Brunie et al. (1990) reported a crystallographic study of *E. coli* MetRs tryptic fragment complexed with ATP. The ribose of ATP is deduced to be in C2′ *endo* conformation. No other features of the adenosine conformation were described, presumably because of insufficient resolution. Other aminoacyl tRNA synthetases for which x-ray structures of ATP (or ATP analog) complexes have been investigated include the glutaminyl (Perona et al., 1993), aspartyl (Cavarelli et al., 1994), and seryl tRNA synthetases (Belrhali et al., 1994). Measurement of the glycosidic orientations by downloading the structures from a protein data bank yields 52° and 60°, respectively, for AMP and ATP

bound to glutaminyl synthetase, 72° for ATP bound to the aspartyl enzyme, and 32° for AMP bound to the seryl enzyme. The x-ray data thus yield a broad range of values for the aminoacyl tRNA synthetases, as it did for kinases. The NMR measurements are made on enzyme-substrate complexes in aqueous solutions under conditions in which the enzymatic reactions readily occur and enzyme-bound equilibrium mixtures can be observed (Fayat et al., 1980), rather than in the crystalline state, in which they may or may not. Thus the NMR-determined conformation, within the limitations of the accuracy, is more likely to represent the active form, whereas the crystallization process required for the x-ray measurements may sometimes trap the substrate in an unproductive conformation. On the other hand, the crystallographic studies unravel considerable information regarding the amino acid environment and the functional groups involved in nucleotide binding and in the possible catalytic steps of the activation reaction. Such information is not readily obtained from NMR, especially for proteins heavier than about 20 kDa. A correlation of the x-ray-determined active-site environment of the nucleotide with the NMR-determined nucleotide conformation is likely to shed considerable light on the catalytic mechanism of the activation reaction.

The authors wish to thank Dr. Sylvain Blanquet, Ecole Polytechnique, Palaiseau, France, for his kind and continued interest in and support for this research, and Dr. Daniel H. Robertson at the Facility for Computational Molecular and Biomolecular Science, IUPUI, for helpful suggestions.

This work was supported in part by grants from National Institutes of Health (GM 43966) and IUPUI.

REFERENCES

Abele, U., and G. E. Schulz. 1995. High-resolution structures of adenylate kinase from yeast ligated with inhibitor AP_5A, showing the pathway of phosphoryl transfer. *Protein Sci.* 4:1262–1271.

Altona, C., and M. Sundaralingam. 1972. Conformational analysis of the sugar ring in nucleosides and nucleotides. A new description using the concept of pseudorotation. *J. Am. Chem. Soc.* 94:8205–8212.

Belrhali, H., A. Yaremchuk, M. Tukalo, K. Larsen, C. Berthet-Colominas, R. Leberman, B. Beijer, B. Sproat, J. Als-Nielsen, G. Grubel, J.-F. Legrand, M. Lehmann, and S. Cusack. 1994. Crystal structures at 2.5 angstrom resolution of seryl-tRNA synthetase complexed with two analogs of seryl adenylate. *Science.* 263:1432–1436.

Brooks, B. R., R. E. Bruccoleri, B. D. Olafson, D. J. States, S. Swaminathan, and M. Karplus. 1983. CHARM: a program for macromolecular energy, minimization, and dynamics calculations. *J. Comp. Chem.* 4:187–217.

Brunie, S., C. Zelwer, and J.-L. Risler. 1990. Crystallographic study at 2.5 Å resolution of the interaction of methionyl-tRNA synthetase from *Escherichia coli* with ATP. *J. Mol. Biol.* 216:411–424.

Campbell, A. P., and B. D. Sykes. 1991. Theoretical evaluation of the two-dimensional transferred nuclear Overhauser effect. *J. Magn. Reson. Imaging.* 93:77–92.

Cassio, D., and J.-P. Waller. 1971. Modification of methionyl-tRNA synthetase by proteolytic cleavage and properties of the trypsin-modified enzyme. *Eur. J. Biochem.* 20:283–300.

Cavarelli, J., G. Eriani, B. Rees, M. Ruff, M. Boeglin, A. Mitschler, F. Martin, J. Gangloff, J.-C. Thierry, and D. Moras. 1994. The active site of yeast aspartyl-tRNA synthetase: structural and functional aspects of the aminoacylation reaction. *EMBO J.* 13:327–337.

De Leeuw, H. P. M., C. A. G. Haasnoot, and C. Altona. 1980. Empirical correlations between conformational parameters in β-D-furanoside fragments derived from a statistical survey of crystal structures of nucleic acid constituents. *Isr. J. Chem.* 20:108–126.

Eriani, G., M. Delarue, O. Poch, J. Gangloff, and D. Moras. 1990. Partition of tRNA synthetases into two classes based on mutually exclusive sets of sequence motifs. *Nature.* 347:203–206.

Fayat, G., S. Blanquet, B. D. Nageswara Rao, and M. Cohn. 1980. ^{31}P NMR of the reversible methionine activation reaction catalyzed by methionyl-tRNA synthetase of *Escherichia coli*. *J. Biol. Chem.* 255: 8164–8169.

Fayat, G., M. Fromant, and S. Blanquet. 1977. Couplings between the sites for methionine and adenosine 5′-triphosphate in the amino acid activation reaction catalyzed by trypsin-modified methionyl-transfer RNA synthetase from *Escherichia coli*. *Biochemistry.* 16:2570–2579.

Fayat, G., and J.-P. Waller. 1974. The mechanism of action of methionyl-tRNA synthetase from *Escherichia coli*. *Eur. J. Biochem.* 44:335–342.

Fourmy, D., T. Meinnel, Y. Mechulam, and S. Blanquet. 1993. Mapping of the zinc binding domain of *Escherichia coli* methionyl-tRNA synthetase. *J. Mol. Biol.* 231:1068–1077.

Hecht, S. M. 1979. 2′-OH *vs.* 3′-OH specificity in tRNA aminoacylation. *In* Transfer RNA: Structure, Properties and Recognition. R. R. Shimmel, D. Soll, and J. N. Abelson, editors. Cold Spring Harbor Laboratory, New York. 345–360.

Higgins, C. F., I. D. Hiles, G. P. C. Salmonal, D. R. Gill, J. A. Downie, I. J. Evans, I. B. Holland, L. Gray, S. D. Buckel, A. W. Bell, and M. A. Hermodson. 1986. A family of related ATP-binding subunits coupled to many distinct biological processes in bacteria. *Nature.* 323:448–450.

Hirel, P.-H., F. Lévêque, P. Mellot, F. Dardel, M. Panvert, Y. Mechulam, and G. Fayat. 1988. Genetic engineering of methionyl-tRNA synthetase: in vitro regeneration of an active synthetase by proteolytic cleavage of a methionyl-tRNA synthetase-β-galactosidase chimeric protein. *Biochimie.* 70:773–782.

Hountondji, C., P. Dessen, and S. Blanquet. 1993. The SKS AND KMSKS signature of Class I amino acyl tRNA synthetases correspond to the GKT/S sequence characteristic of the ATP-binding site of many proteins. *Biochimie.* 75:1137–1142.

Jackson, P. L., H. N. B. Moseley, and N. R. Krishna. 1995. Relative effects of protein-mediated and ligand-mediated spin-diffusion pathways on transferred NOESY, and implications on the accuracy of the bound ligand conformation. *J. Magn. Reson. Imaging.* B107:289–292.

Jarori, G. K., N. Murali, and B. D. Nageswara Rao. 1994. Two-dimensional transferred nuclear Overhauser effect spectroscopy study of the conformation of MgATP bound at the active and ancillary sites of rabbit muscle pyruvate kinase. *Biochemistry.* 33:6784–6791.

Jarori, G. K., N. Murali, and B. D. Nageswara Rao. 1995. Conformation of MgATP bound to 5-phospho-α-D-ribose 1-diphosphate synthetase by two-dimensional transferred nuclear Overhauser effect spectroscopy. *Eur J. Biochemistry.* 230:517–524.

Kalk, A., and H. J. C. Berendson. 1976. Proton magnetic relaxation and spin diffusion in proteins. *J. Magn. Reson. Imaging.* 24:343–366.

Keepers, J. W., and T. L. James. 1984. A theoretical study of distance determinations from NMR. Two-dimensional nuclear Overhauser spectra. *J. Magn. Reson. Imaging.* 57:404–426.

Koning, T. M. G., R. Boelens, and R. Kaptein. 1990. Calculation of the nuclear Overhauser effect and the determination of proton-proton distances in the presence of internal motions. *J. Magn. Reson. Imaging.* 90:111–123.

Kumar, A., R. R. Ernst, and K. Wüthrich. 1980. A two-dimensional nuclear Overhauser enhancement (2D NOE) experiment for the elucidation of complete proton-proton cross-relaxation networks in biological macromolecules. *Biochem. Biophys. Res. Commun.* 95:1–6.

Landy, S. B., and B. D. Nageswara Rao. 1989. Dynamical NOE in multi-spin systems undergoing chemical exchange. *J. Magn. Reson. Imaging.* 81:371–377.

Landy, S. B., B. D. Ray, P. Plateau, K. B. Lipkowitz, and B. D. Nageswara Rao. 1992. Conformation of MgATP bound to nucleotidyl and phosphoryl transfer enzymes ^1H-transferred NOE measurements on complexes of methionyl tRNA synthetase and pyruvate kinase. *Eur. J. Biochem.* 205:59–69.

Lee, W., and N. R. Krishna. 1992. Influence of conformational exchange slow on the chemical shift scale on 2D NOESY spectra of biomolecules existing in multiple conformations. *J. Magn. Reson. Imaging.* 98:36–48.

London, R. E., M. E. Perlman, and D. G. Davis. 1992. Relaxation-matrix analysis of the transferred nuclear Overhauser effect for finite exchange rates. *J. Magn. Reson. Imaging.* 97:79–98.

Macura, S., Y. Huang, D. Sueter, and R. R. Ernst. 1981. Two-dimensional chemical exchange and cross-relaxation spectroscopy of coupled nuclear spins. *J. Magn. Reson. Imaging.* 43:259–281.

McPhillips, T. M., B. T. Hsu, M. A. Sherman, M. T. Mas, and D. C. Rees. 1996. Structure of the R65Q mutant of yeast 3-phosphoglycerate kinase complexed with Mg-AMP-PNP and 3-phospho-D-glycerate. *Biochemistry.* 35:4118–4127.

Meinnel, T., Y. Mechulam, and S. Blanquet. 1995. Aminoacyl-tRNA synthetases: occurrence, structure and function. *In* tRNA: Structure, Biosynthesis and Function. D. Soll, D. Raj Bhandary, and V. Raj Bhandary, editors. American Society for Microbiology, Washington, DC.

Meinnel, T., Y. Mechulam, D. LeCorre, M. Panvert, S. Blanquet, and G. Fayat. 1991. Selection of suppressor methionyl-tRNA synthetases: mapping the tRNA anticodon binding site. *Proc. Natl. Acad. Sci. USA.* 88:291–295.

Mellot, P., Y. Mechulam, D. LeCorre, S. Blanquet, and G. Fayat. 1989. Identification of an amino acid region supporting specific methionyl-tRNA synthetase: tRNA recognition. *J. Mol. Biol.* 208:429–443.

Moseley, H. N. B., E. V. Curto, and N. R. Krishna. 1995. Complete relaxation and conformation exchange matrix (CORCEMA) analysis of NOESY spectra of interaction systems: two-dimensional transferred NOESY. *J. Magn. Reson. Imaging.* B108:243–261.

Murali, N., G. K. Jarori, S. B. Landy, and B. D. Nageswara Rao. 1993. Two-dimensional transferred nuclear Overhauser effect spectroscopy (TRNOESY) studies of nucleotide conformations in creatine kinase complexes: effects due to nonspecific binding. *Biochemistry.* 32: 12941–12948.

Murali, N., G. K. Jarori, and B. D. Nageswara Rao. 1994. Two-dimensional transferred nuclear Overhauser effect spectroscopy (TRNOESY) studies of nucleotide conformations in arginine kinase complexes. *Biochemistry.* 33:14227–14236.

Nageswara Rao, B. D., and B. D. Ray. 1992. ^{13}C NMR line shapes of [2-^{13}C]ATP in enzyme complexes and viscous solutions: glycosidic rotation persists at high viscosities and is arrested in enzyme complexes. *J. Am. Chem. Soc.* 114:1566–1573.

Ni, F., and Y. Zhu. 1994. Accounting for ligand-protein interaction in the relaxation-matrix analysis of transferred nuclear Overhauser effects. *J. Magn. Reson. Imaging.* B102:180–184.

Nirmala, N. R., G. M. Lippens, and K. Hallenga. 1992. Theory and experimental results of transfer NOE experiments. II. The influence of residual mobility and relaxation centers inside the protein on the size of transfer NOEs. *J. Magn. Reson. Imaging.* 100:25–42.

Perona, J. J., M. A. Rould, and T. A. Steitz. 1993. Structural basis for transfer RNA aminoacylation by *Escherichia coli* glutaminyl-tRNA synthetase. *Biochemistry.* 32:8758–8771.

Rosevear, P. R., H. N. Bramson, C. O'Brian, E. T. Kaiser, and A. S. Mildvan. 1983. Nuclear Overhauser effect studies of the conformation of tetraaminecobalt (III)-adenosine 5′-triphosphate free and bound to bovine heart protein kinase. *Biochemistry.* 22:3439–3447.

Rosevear, P. R., P. Desmeules, G. L. Kenyon, and A. S. Mildvan. 1981. Nuclear magnetic resonance studies of the role of histidine residues at the active site of rabbit muscle creatine kinase. *Biochemistry.* 20: 6155–6164.

Rosevear, P. R., V. M. Powers, D. Dowhan, A. S. Mildvan, and G. L. Kenyon. 1987. Nuclear Overhauser effect studies of the conformation of magnesium adenosine 5′-triphosphate bound to rabbit muscle creatine kinase. *Biochemistry.* 26:5338–5344.

Sanger, W. 1984. Principles of Nucleic Acid Structure. C. R. Cantor, editor. Springer-Verlag, New York. 9–28.

Schulz, G. E. 1992. Binding of nucleotides by proteins. *Curr. Opin. Struct. Biol.* 2:61–67.

Smith, C. A., and I. Rayment. 1996. Active site comparisons highlight structural similarities between myosin and other P-loop proteins. *Biophys. J.* 70:1590–1602.

States, D. J., R. A. Haberkorn, and D. J. Ruben. 1982. A two-dimensional nuclear Overhauser experiment with pure absorption phase in four quadrants. *J. Magn. Reson. Imaging.* 48:286–292.

Traut, T. W. 1994. The functions and consensus motifs of nine types of peptide segments that form different types of nucleotide-binding sites. *Eur. J. Biochem.* 222:9–19.

Williams, J. S., and P. R. Rosevear. 1991a. Nuclear Overhauser effect studies on the conformations of Mg(α,β-methylene)ATP bound to *Escherichia coli* methionyl-tRNA synthetase. *J. Biol. Chem.* 266:2089–2098.

Williams, J. S., and P. R. Rosevear. 1991b. Nuclear Overhauser effect studies of the conformations of μg (α,β-methylene) ATP bound to *Escherichia coli* isoleucyl-tRNA synthetase. *Biochem. Biophys. Res. Commun.* 176:682–689.

Zheng, J., and C. B. Post. 1993. Protein indirect relaxation effects in exchange-transferred NOESY by a rate-matrix analysis. *J. Magn. Reson. Imaging.* B101:262–270.